International Journal of Electrical, Electronic and Communication Sciences
ISSN: 2517-9438
Vol:3, No:9, 2009

Modeling and Simulation of Position Estimation of Switched Reluctance Motor with Artificial Neural Networks

Oguz Ustun, and Erdal Bekiroglu

Abstract**—**In the present study, position estimation of switched reluctance motor (SRM) has been achieved on the basis of the artificial neural networks (ANNs). The ANNs can estimate the rotor position without using an extra rotor position sensor by measuring the phase flux linkages and phase currents. Flux linkage-phase current-rotor position data set and supervised backpropagation learning algorithm are used in training of the ANN based position estimator. A 4-phase SRM have been used to verify the accuracy and feasibility of the proposed position estimator. Simulation results show that the proposed position estimator gives precise and accurate position estimations for both under the low and high level reference speeds of the SRM.

Keywords**—**Artificial neural networks**,** modeling and simulation, position observer, switched reluctance motor.

I. INTRODUCTION

THE switched reluctance motors are simple, low cost, and robust motors that make them favorable for variable servo drive applications. However, torque ripple, acoustic noise and rotor position sensor requirements are the main disadvantages of the motor [1-2]. Several methods have been introduced to achieve position sensorless operation of the SRM in the recent years. The main principle used in the position estimation is the derivation of rotor position information from the stator circuit measurements or their derived parameters [3]. These parameters are mainly stator phase voltages and currents. The flux linkage is derived from these parameters. Position estimation is achieved by using flux linkage and phase current. The various sensorless methods published in the literature have been extensively classified in the Ref. [4].

The capability of ANNs makes them ideal solution for estimation of parameters, modeling nonlinear characteristics, and compensating disturbances and uncertainties in control systems. Recently, ANN techniques have taken place in real-time control and modeling applications owing to increase in microprocessor/microcontroller speed and capabilities. Various studies about sensorless parameter estimation and control of SRMs using intelligent techniques have been reported in the literature. Neural networks based sensorless position estimation of SRMs has been presented in [5-8]. Sensorless position control of SRM based on ANN without using flux estimator is reported in [9]. Current-flux-rotor position look-up table based position sensorless operation of SRM is given in [10]. NN is used to construct the look-up table in that study. Rotor position estimation of a SRM involving flux current method using adaptive network fuzzy inference system (ANFIS) is presented in [11]. An approach of single neuron PID control for position sensorless switched reluctance motors (SRM) based on radial basis function NN is proposed in [12]. ANN and ANFIS based sensorless position estimation techniques with digital flux linkage calculation are presented in [13]. Sensorless control of single switch-based switched reluctance motor drive using neural network has been implemented in [14-15].

The aim of this study is to develop a position estimator that can be easily used for the SRM position control applications. A sensorless position estimation of the SRM has been built on the basis of ANNs. Position of the SRM is obtained from the ANN model as a function of the phase current and the flux linkage. The node numbers of hidden layers have been chosen as possible as at minimum level. Taking into account the real applications, a 2-3-3-1 multilayer feedforward NN (MFNN) structure have been designed in the study to decrease the process time. As a result, the computational load of processor has been decreased. Simulation studies have been performed to present validity and applicability of the proposed position observer. The obtained results reveal that the developed position observer gives effective and accurate results.

II. ANN-BASED ROTOR POSITION ESTIMATOR

Modeling and simulation studies performed in this study to design the position observer are built on the 4 phases, 5.5HP, 1500 rpm, and 8/6 poles SRM given in Fig. 1.

Oguz Ustun is with the Abant Izzet Baysal University, Faculty of Engineering and Architecture, Department of Electrical and Electronics Engineering, Bolu, 14280 Turkey (e-mail: oguzustun@ibu.edu.tr).

Erdal Bekiroglu is with Abant Izzet Baysal University, Faculty of Engineering and Architecture, Department of Electrical and Electronics Engineering, Bolu, 14280 Turkey (corresponding author phone: +90-374-2534640; fax: +90-374-2534558; e-mail: bekiroglu_e@ibu.edu.tr).

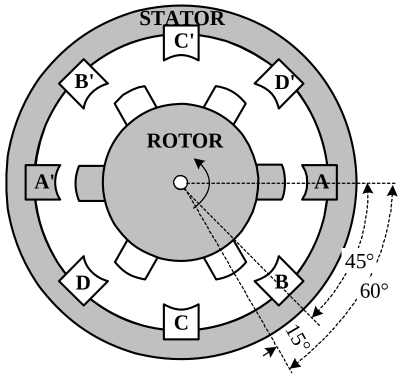

Fig. 1 Cross section of 8/6 poles SRM

The network structure shown in Fig. 2 is used for estimating the rotor position by using ANN. The network is similar to the network model given in [16]. The inputs of the networks i_j and ψ_j are the phase current and the flux linkage data are obtained from the non-linear full model of the SRM [17]. The output of network is the actual rotor position per phase $\hat{\theta}_j$ computed according to the inputs. θ_j is the desired rotor position per phase, while *e* is the error between actual and desired rotor position values. The network is composed of 4 layers: an input layer (P), two hidden layers (R, S), and an output layer (T).

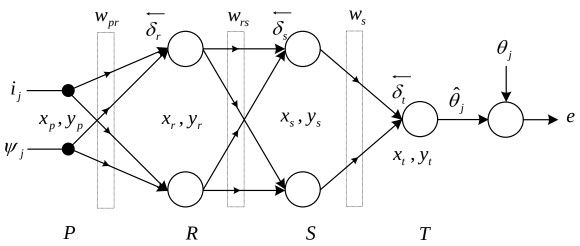

Fig. 2 Architecture of the neural network for modeling of the inductance and flux linkage

In nodes at the *R*, *S*, and *T*, the output of the nodes is calculated by using activation function given as follows;

$$y(x) = exp\left(-\left(\frac{x-c}{\sigma}\right)^2\right) \quad (1)$$

Here, *x* represents input of the nodes, *y* represents output of the nodes related to *x*, *c* center of Gaussian function, and σ its width. Feedforward model of the layers can be described as follows.

A. Feedforward Algorithm

P ***layer:*** It is the input layer and the entry of this layer, i_j and ψ_j are the values of the current and flux linkage data, respectively. The inputs and the outputs of this layer are obtained as follows.

$$x_p = \{i_j, \psi_j\}, \text{and } y_p = x_p \text{ where } p = 0...P \quad (2)$$

R ***layer:*** It is the first hidden layer. The inputs and the outputs of this layer are obtained as follows.

$$x_r = \sum_{p=0}^{P} y_p.w_{pr}\text{ , and } y_r = y(x_r) \text{ where } r = 0...R \quad (3)$$

S ***layer:*** It is the second hidden layer. The inputs and the outputs of this layer are obtained as follows.

$$x_s = \sum_{r=0}^{R} y_r.w_{rs}\text{ ,and } y_s = y(x_s) \text{ where } s = 0...S \quad (4)$$

T ***layer:*** It is the output layer. The inputs and the outputs of this layer are obtained as follows.

$$x_t = \sum_{s=0}^{S} y_s.w_s\text{ , and } y_t = y(x_t) \quad (5)$$

While the terms above layers are combined; inductance model can be expressed as follows,

$$\hat{\theta}_j = y\left(\sum_s^S y\left(\sum_{r=0}^R y\left(\sum_{p=0}^P y_p.w_{pr}\right).w_{rs}\right).w_s\right) \quad (6)$$

The estimated rotor position model is obtained as a result of the feedforward algorithm. Once the feedforward algorithm has been completed, the backpropagation learning algorithm is realized for the optimization of the weights in the network.

B. Backpropogation Learning Algorithm

To describe the online learning algorithm of the ANN using the supervised gradient decent method, first the energy function *E* is chosen as follows [16],

$$E(k) = \frac{1}{2}e^2(k)\text{, where } k = 1,\cdots,K \quad (7)$$

K denotes total number of input-output patterns. Error value for each pattern,

$$e(k) = \theta_j(k) - \hat{\theta}_j(k) \quad (8)$$

where $\theta_j(k)$ is the desired value $\hat{\theta}_j(k)$ actual value. Accordingly, all the weights in network are adjusted as follows,

T ***layer:*** As no weight is adjusted on this layer, error value in the network output is backpropagated by making use of chain rule.

S ***layer:*** Weight changes on this layer Δw_s are calculated as follows,

$$\Delta w_s = \eta_s \left(-\frac{\partial E}{\partial w_s} \right) = \eta_s \left(-\frac{\partial E}{\partial e} \frac{\partial e}{\partial \hat{\psi}_j} \frac{\partial \hat{\psi}_j}{\partial y_t} \frac{\partial y_t}{\partial x_t} \frac{\partial x_t}{\partial w_s} \right) \tag{9}$$

R ***layer:*** Weight changes on this layer Δw_{rs} are calculated as follows,

$$\Delta w_{rs} = \eta_{rs} \left(-\frac{\partial E}{\partial w_{rs}} \right) = \eta_{rs} \left(-\frac{\partial E}{\partial e} \frac{\partial e}{\partial \hat{\psi}_j} \frac{\partial \hat{\psi}_j}{\partial y_t} \frac{\partial y_t}{\partial x_t} \frac{\partial x_t}{\partial y_s} \frac{\partial y_s}{\partial x_s} \frac{\partial x_s}{\partial w_{rs}} \right) \tag{10}$$

P ***layer:*** Weight changes on this layer Δw_{pr}^{ψ} are calculated as follows,

$$\Delta w_{pr} = \eta_{pr} \left(-\frac{\partial E}{\partial w_{pr}} \right) = \eta_{pr} \left(-\frac{\partial E}{\partial e} \frac{\partial e}{\partial \hat{\psi}_j} \frac{\partial \hat{\psi}_j}{\partial y_t} \frac{\partial y_t}{\partial x_t} \frac{\partial x_t}{\partial y_s} \frac{\partial y_s}{\partial x_s} \frac{\partial x_s}{\partial y_r} \frac{\partial y_r}{\partial x_r} \frac{\partial x_r}{\partial w_{pr}} \right) \tag{11}$$

η_s , η_{rs} , and η_{pr} are learning coefficients. Weight changes Δw_s , Δw_{rs} , and Δw_{pr} are obtained as follows,

$$w_s(k+1) = w_s(k) + \Delta w_s \tag{12}$$

$$w_{rs}(k+1) = w_{rs}(k) + \Delta w_{rs} \tag{13}$$

$$w_{pr}(k+1) = w_{pr}(k) + \Delta w_{pr} \tag{14}$$

In the beginning of network training, weight values can be chosen in relation with previous data or they can be chosen random as well. In this study, the initial values [0,1] of weights are given randomly, and these values are limited at these values during the training. Learning coefficients are also selected in [0,1] interval.

III. Simulation Results

Simulation studies have been achieved for testing the performance of the ANN based position observer described in the Section II. Simulation results are given for the low and the high speed references, 30 rad/s and 150 rad/s, respectively. The reference current has been fixed as 9 A. The obtained simulation results have been given in Figs. 3-10. Actual and desired rotor position graphics under 30-150 rad/s speed reference is given in Fig. 3. The current and speed graphics have been given in Fig. 4 and Fig. 5, respectively. Actual and desired rotor position graphics for the 30 rad/s reference speed have been given in Fig. 6, and the current waveform at this situation has been given in Fig. 7. As seen from the figure, the actual rotor position follows the desired rotor position precisely. The phase current is 9 A as it is fixed at the reference stage. Actual and desired rotor position graphics for the 150 rad/s reference speed have been given in Fig. 8, and the current waveform at this situation has been given in Fig. 9. As seen from the figure, the actual rotor position follows the desired rotor position precisely. Due to increase in the reference speed, the phase current has decreased. The phase current is 2.65 A at this operating condition. As seen form the position graphics, actual positions are following the desired positions accurately for both the low and the high reference speeds. There is a slightly difference between actual and desired positions only at the points of phase current changes. These changes caused from the phase transient points. Phase currents are given for the 60º mechanical rotor position (one pole movement) to show the effect of the phase changes and the switching angles (Fig. 10). As seen from the figure, the effect of the each phase is 15º.

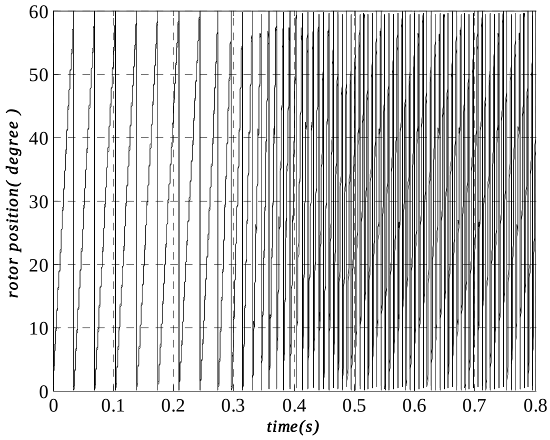

Fig. 3 Actual and desired rotor position for 30-150 rad/s

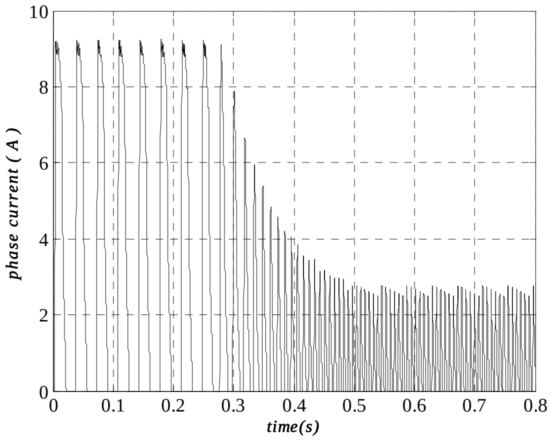

Fig. 4 Phase current for 30-150 rad/s

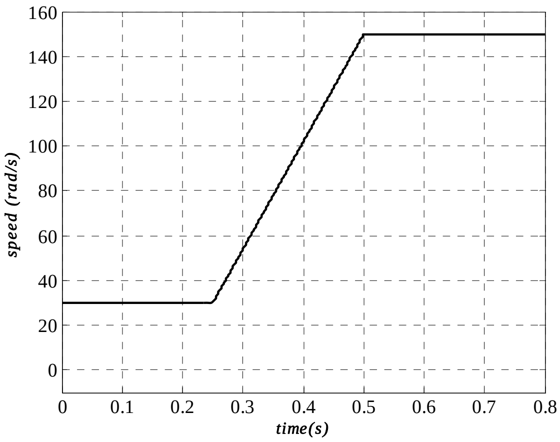

Fig. 5 Rotor speed

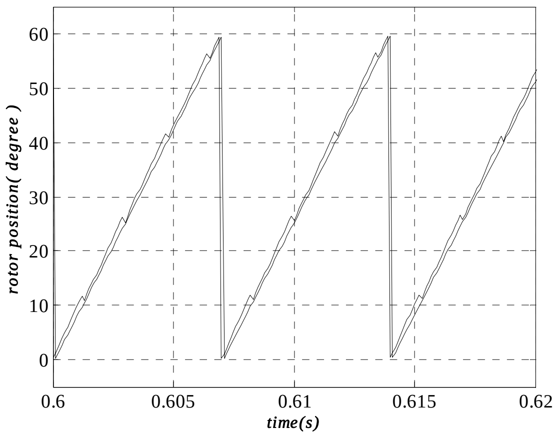

Fig. 8 Actual and desired rotor position for 150 rad/s

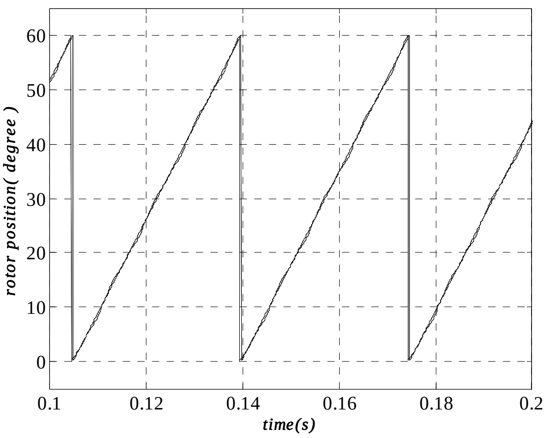

Fig. 6 Actual and desired rotor position for 30 rad/s

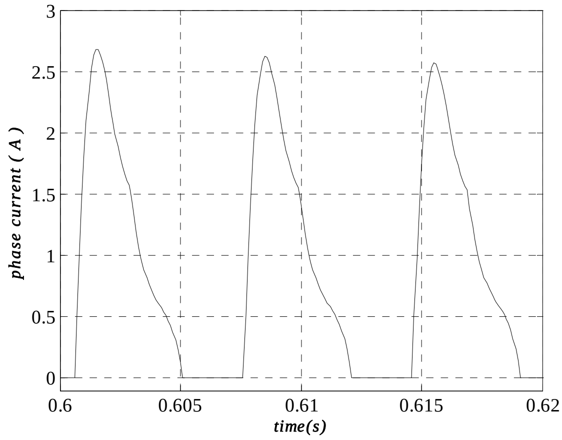

Fig. 9 Phase current for 30 rad/s

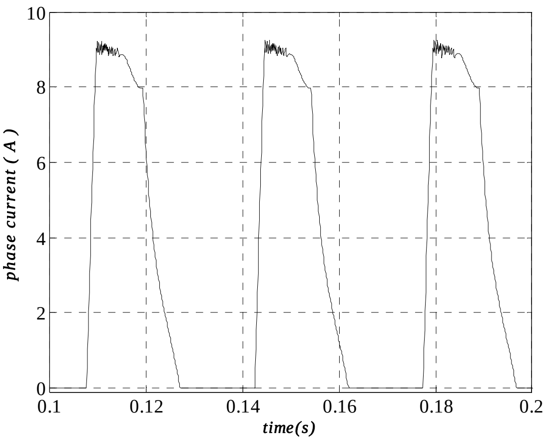

Fig. 7 Phase current for 30 rad/s

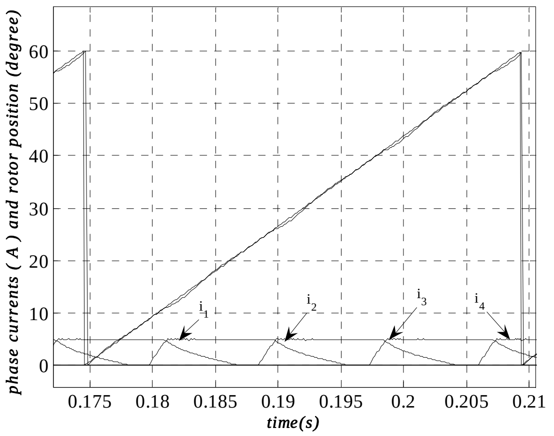

Fig. 10 Phase currents and rotor position

IV. Conclusion

A sensorless position observer has been designed for the 8/6 SRM. ANN based nonlinear model including feedforward and backpropagation learning algorithms has been constructed to achieve position estimation of the SRM. Position of the SRM is obtained from the ANN model as a function of phase current and flux linkage. The calculation process has been taken into account to apply the developed model on the real applications effectively. Simulation studies have been performed to approve and show capability of the ANN based sensorless position estimator. The simulation results show that the developed scheme gives superior position characteristics of the SRM.

References

[1] R. Krishnan, *Switched Reluctance Motor Drives: Modeling, Simulation, Analysis, Design, and Applications*. Boca Raton, FL: CRC Press, Jun. 2001.

[2] E. Mese, “A rotor position estimator for switched reluctance motors using CMAC”, *Energy Conversion and Management*, 44 (2003) 1229–1245.

[3] E. Mese and D. A. Torrey, “An approach for sensorless position estimation for switched reluctance motors using artificial neural networks,” *IEEE Trans. Power Electron.*, vol. 17, no. 1, Jan. 2002, pp. 66–75.

[4] M. Ehsani, and B. Fahimi, “Elimination of position sensors in switched reluctance motor: State of the art and future trends,” *IEEE Trans. Ind. Electron.*, vol. 49, no. 1, Feb. 2002, pp. 40-47.

[5] D.S. Reay, Y. Dessouky, and B.W. Williams, “The use of neural networks to enhance sensorless position detection in switched reluctance motors”, *IEEE International Conference on Systems, Man, and Cybernetics*, 1998, pp. 1774-1778.

[6] H. S. Ooi and T. C. Green, “Simulation of neural networks to sensorless control of switched reluctance motor,” in *Proc. IEEE Power Electron. Variable Speed Drives*, Sep. 1998, pp. 281–286.

[7] D. S. Reay and B. W. Williams, “Sensorless position detection using neural networks for the control of switched reluctance motors,” in *Proc. IEEE Int. Conf. Control Appl.*, vol. 2, Aug. 1999, pp.1073–1077.

[8] T. Lachman, T. R. Mohamad, and S. P. Teo, “Sensorless position estimation of switched reluctance motors using artificial neural networks,” in *Proc. IEEE Int. Conf. Robot., Intell. Syst. Signal Process.*, vol. 1, Oct. 2003, pp. 220–225.

[9] B. Enayati, and S.M. Saghaiannejad, “Sensorless position control of switched reluctance motors based on artificial neural networks”, *IEEE ISIE 2006*, July 9-12, 2006, Montreal, Quebec, Canada, pp. 2266-2271.

[10] W.S. Baik, M.H. Kim, N.H. Kim, and D.H. Kim, “Position sensorless control system of srm using neural network,” *Proc. IEEE PESC*, vol. 5, Jun. 2004, pp. 3471–3475.

[11] S. Paramasivam, R. Arumugam, B. Umaniaheswari, “Accurate rotor position estimation for switched reluctance motor using ANFIS”, *Conference on Convergent Technologies for Asia-Pacific Region TENCON 2003*, Volume 4, 15-17 Oct. 2003 pp. 1493-1497.

[12] T. Shi, C. Xia, M. Wang and Qian Zhang, “Single neural PID control for sensorless switched reluctance motor based on RBF neural network”, *Proceedings of the 6th World Congress on Intelligent Control and Automation*, June 21-23, 2006, Dalian, China, pp. 8069-8073.

[13] S. Paramasivam, S. Vijayan, M. Vasudevan, R. Arumugam, and Ramu Krishnan, “Real-time verification of AI based rotor position estimation techniques for a 6/4 pole switched reluctance motor drive”, *IEEE Transactions on Magnetics*, vol. 43, no. 7, July 2007, pp. 3209-3222.

[14] C. Hudson, N:S. Lobo, R. Krishnan, “Sensorless control of single switch based switched reluctance motor drive using neural network”, *The 30th Annual Conference of the IEEE Industrial Electronics Society*, November 2-6, Busan, Korea, 2004, pp. 2349-2354.

[15] C. A. Hudson, N. S. Lobo, and R. Krishnan, “Sensorless Control of Single Switch-Based Switched Reluctance Motor Drive Using Neural Network”, *IEEE Transactions On Industrial Electronics*, vol. 55, no. 1, January 2008, pp. 321-329.

[16] O. Ustun, “Measurement and real-time modeling of inductance and flux linkage in switched reluctance motors”, *IEEE Transactions on Magnetics*, In press.

[17] O. Ustun, “A nonlinear full model of switched reluctance motor with artificial neural network”, *Energy Conversion and Management*, doi:10.1016/j.enconman.2009.05.025.

Oguz Ustun (M’07) and received his BSc, MSc, and PhD degrees in the Electrical Technologies Education from the Gazi University. He worked as a research assistant at the Gazi University between 1997 and 2007. He is currently assistant professor at the Department of Electrical and Electronics Engineering, Faculty of Engineering and Architecture, Abant Izzet Baysal University. His research interests are artificial neural networks, genetic algorithms, digital signal processors, drive and control of electrical machines.

Erdal Bekiroglu (M’08) received his BSc, MSc, and PhD degrees in the Electrical Technologies Education from the Gazi University. He worked as a research assistant at the Gazi University between 1996 and 2003. He is currently assistant professor at the Department of Electrical and Electronics Engineering, Faculty of Engineering and Architecture, Abant Izzet Baysal University. His research interests are computer-controlled systems, digital signal processors, special electrical motors, drive and control of electrical machines.